PNAS
www.pnas.org

Supplementary Information for

Scd1 controls de novo beige fat biogenesis through succinate-dependent regulation of mitochondrial complex II

Keli Liu[1,2], Liangyu Lin[1], Qing Li[1], Yueqing Xue[1], Fanjun Zheng[1], Guan Wang[1], Chunxing Zheng[1], Liming Du[1], Mingyuan Hu[1], Yin Huang[1], Changshun Shao[3], Xiangyin Kong[1], Gerry Melino[4], Yufang Shi[1,2,3,*], Ying Wang[1,*]

Corresponding author: Ying Wang and Yufang Shi
Email: yingwang@sibs.ac.cn (Y.W.), yufangshi@sibs.ac.cn (Y.S.)

This PDF file includes:

Supplementary text
Figures S1 to S8
Tables S1
Legends for Datasets S1 to S3

www.pnas.org/cgi/doi/10.1073/pnas.1914553117

Supplementary Information Text

Materials and methods.

Isolation, Culture and Differentiation of Mouse ADSCs. Inguinal adipose tissues were isolated from mice, cut into pieces, and digested with collagenase at 37°C. The cells were collected by centrifugation at 600 × g for 5 min and resuspended with PBS. After filtrated with cell strainer, cells were seeded into plates and cultured for 48 h. Adherent preadipocytes were expanded in culture medium containing low-glucose DMEM (Gibco) and 10% fetal bovine serum (FBS), and maintained in a humidified incubator at 37°C with 5% CO_2 supply. For white adipocyte differentiation, confluent cells were cultured in adipogenic induction medium (high-glucose DMEM with 10% FBS, 0.5 mM isobutyl methylxanthine, 50 μM indomethacin, 1 μM dexamethasone and 10 μg/ml insulin) for 3 days. Culture medium was then replaced with maintenance medium (high-glucose DMEM supplemented with10 μg/mL insulin and 10% FBS) until harvest. For brown/beige adipocyte differentiation, confluent cells were cultured in adipogenic induction medium (high-glucose DMEM medium with 10% FBS, 0.5 mM isobutyl methylxanthine, 125 nM indomethacin, 1 μM dexamethasone, 1 μM rosiglitazone, 5 nM triiodothyronine and 10 μg/ml insulin) for 3 days. The medium was then replaced with the maintenance medium (high-glucose DMEM with 1 μM rosiglitazone, 5 nM triiodothyronine, 10 μg/mL insulin and 10% FBS) until harvest.

Metabolic Phenotyping. Eight-week-old mice were fed with a 60% fat diet (Research Diets, D12492i) or a normal chow (NC), housed at room temperature (RT) with a 12 h light-dark cycle, and free to access food and water. Body weight was monitored weekly. Tests for glucose tolerance and insulin resistance were performed by intraperitoneal injection of D-glucose (2 g/kg body weight) or insulin (0.75 U/kg body weight) to 16 h- and 8 h- fasting mice respectively, with a measurement of glucose in serum at different time-points before and after injection. Lean mass and fat mass of mice were detected using the Bruker Minispec Mq7.5 Live Mice Analyzer (Bruker Optics, Inc.). Mouse activity, food intake and energy expenditure were monitored using a Comprehensive Lab Animal Monitoring System (CLAMS, Columbus Instruments). Mice were housed under an inverse 12 h light-dark cycle, with ad-lib access to food and water.

***In vivo* Adipogenesis.** ADSCs were isolated from RF-tracing mice as previously described. After mixed with cold PBS, ADSCs were immediately mixed with matrigel. The mixture was implanted into subcutaneous in the chest with a cooled syringe. Mice were placed on a heating plate to quickly warm the mixture. Four weeks later, mice were sacrificed, and matrigel was isolated for further analysis.

Histological Analysis. Adipose tissue was fixed in 4% paraformaldehyde, then embedded in paraffin and cut into slices. Hematoxylin and eosin (H&E) staining was performed according to standard protocols. For immunohistochemistry, sections were subjected to antigen-retrieval in citrate acid buffer at 95°C for 20 min. After blocking with 5% BSA, sections were incubated with rabbit anti-Ucp1 (Abcam) at 4°C overnight, followed by incubation with HRP-conjugated secondary antibody in PBS at room temperature for 1 h and finally stained with DAB substrate. For Oil-Red O staining, cells were fixed with 10% formalin for 1 h and stained with 2 mg/ml Oil-Red O (Sigma-Aldrich) in a mixture of isopropanol and H_2O at a ratio of 3:2 for 15 min. For whole-mount staining, matrigel was performed as described previously (1). Briefly, matrigel was fixed with 4% paraformaldehyde and permeabilized with 1% TritonX-100. After blocking with 5% BSA, matrigel was stained with rabbit anti-Ucp1 (Abcam) overnight, followed by incubation with goat anti-rabbit IgG conjugated with Alexa Fluor 647 (Thermo Fisher Scientific) for 1 h. The nuclei were stained with DAPI (Thermo Fisher Scientific). The samples were observed under confocal fluorescence microscopy (ZEISS, Germany). Image acquisition and further visualization were performed using ZEN Imaging software (ZEISS, Germany).

Flow Cytometric Analysis. Mouse ADSCs were isolated as the methods mentioned above. Cells were cultured and then digested with trypsin and suspended with PBS. After blocking Fc receptor by anti-CD16/32 Ab, cells were stained with antibodies against cell surface markers. Anti-mouse CD31-PE, anti-mouse CD45-PE, anti-mouse CD140a-PE and anti-mouse Sca-1-PE, anti-mouse CD137-PE from eBioscience (San Diego, CA) were used. For Tbx1 (Abcam) staining, cells were stained with rabbit anti-mouse Tbx1 Ab overnight at 4°C, subsequently stained with

goat anti-rabbit IgG conjugated with Alexa Fluor 647 (Thermo Fisher Scientific) for 30 min. Cells were washed and resuspended in PBS. Cell acquisition was performed on a FACS Calibur flow cytometer. Data were analyzed using FlowJo software.

Cellular Respiration Assay. Cellular oxygen consumption rates (OCR) were performed by an XFe24 extracellular flux analyzer (Seahorse Bioscience). ADSCs were isolated as previously described, and plated on XFe24 cell culture microplate. Cells were cultured in adipogenic medium. Five days later, the medium was replaced with Agilent Seahorse XF Assay Medium, with 25 mM glucose and 1 mM pyruvate addition. The OCR of ADSCs or adipocytes were monitored at both basal level and maximum levels in response to oligomycin (1 μM), FCCP (3 μM), rotenone (100 nM) and antimycin (1 μM).

Mitochondrial Complex Activity Assay. Cells were cultured in 6-well plates under adipogenic condition. At the time-points to detect the mitochondrial complex activity, cells were washed and added with Mitochondria Isolation Buffer (BioVision), and gently scraped. Mitochondria in ADSCs and their differentiated adipocytes were prepared according to the manufacturer instructions of Mammalian Mitochondria Isolation Kit for Tissue and Cultured Cells (BioVision). After detection of the protein concentrations by BCA assay, the isolated mitochondria were examined for the activities of mitochondria complex I, II, III and V according to manufacturer's instruction.

Mitochondrial ROS Measurement. To monitor changes in mitochondrial superoxide, cells were differentiated into mature adipocytes and were loaded with MitoSOX Red (100 nM, Thermo Fisher Scientific) for 10 min. MitoTracker Green (100 nM, Thermo Fisher Scientific) was used to label mitochondria, and incubated for 30 min. The nuclei were stained with Hoechst33342 (Thermo Fisher Scientific). The samples were observed under fluorescence microscopy (ZEISS, Germany). Image acquisition and further visualization were performed using ZEN Imaging software (ZEISS, Germany).

Gene Expression Analysis (RT qPCR and RNA-seq). For gene expression analysis of tissue and cell samples, total RNA was extracted from homogenized tissues or cultured cells using Trizol reagent (Thermo Fisher Scientific), and subjected to reverse transcription using PrimeScript RT master mix (Takara, Kusatsu, Japan). Quantitative real-time PCR was performed with FastStart Universal SYBR Green (Roche Applied Science, Indianapolis, IN) on 7900HT Fast Real-time PCR system (Thermo Fisher Scientific). Detailed primers were listed in the supplemental table (Supplementary Table 3). For RNA-seq, sequencing libraries were generated using NEBNext® UltraTM RNA Library Prep Kit for Illumina® (NEB, USA) following manufacturer's recommendations and index codes were added to attribute sequences to each sample. Then samples were sequenced on the Illumina HiSeq platform. Sequencing reads were mapped to the mouse reference genome using Hisat2 v2.0.5. Normalization and identification of differentially expressed genes was performed using DESeq2. The resulting P-values were adjusted using the Benjamini and Hochberg's approach for controlling the false discovery rate. Genes with an adjusted P-value <0.05 and $|\log2(\text{foldchange})| > 0$ were assigned as differentially expressed. For KEGG pathway enrichment analysis, the list of differential transcripts was analyzed by using clusterProfiler R package.

Immunoblotting Assay. Cultured cells or homogenized tissues were lysed with RIPA lysis buffer (Millipore, Billerica, MA) supplemented with protease inhibitors (Roche Applied Science). Protein concentrations were quantified by Pierce BCA protein assay kit (Thermo Fisher Scientific). After mixed with 5x protein loading buffer, proteins were separated by SDS/PAGE and transferred onto nitrocellulose membrane. Samples were blocked with 5% fat-free milk in TBST and incubated with primary antibody. HRP-linked secondary antibody was used, and a subsequent reaction with ECL substrate was performed to enable detection. Antibodies are listed in the supplemental table.

GC-MS for Fatty Acids Profiles Analysis. Equal mass of inguinal white adipose tissues was isolated and homogenized with cold PBS. Internal standards were then mixed with samples and the mixture was initiated with chloroform and methyl alcohol (1:1, v/v), followed by the addition of sodium chloride. After mixing for 10 min at 2500 rpm, the subnatants were transferred and flushed with nitrogen. Then the samples was dissolved in freshly prepared methylation reagent containing H_2SO_4/MeOH (1:25, v/v) by mixing for 10 min at 2500 rpm and incubated at 80 °C for 2

h. After cooling, samples were mixed with n-hexane by mixing for 10 min at 2500 rpm and then evaporated with nitrogen. The fatty acids extraction was finally dissolved with isooctane and prepared for analysis. Fatty acids analysis was performed on an Agilent 6890N GC with a 5975B inert XL EI/CI MSD (Agilent).

Isotopic metabolic flux analysis. ADSCs were differentiated for 10 days, and then incubated with DMEM (base medium, Sigma) supplied with [U-^{13}C]-glucose or [U-^{13}C]-glutamate for 60 min and 240 min. Samples were harvested and subjected to methanol-acetonitrile-water and chloroform extraction. After drying by centrifugal evaporation, the metabolite residues were dissolved in methanol/water (v/v=1:1) and analyzed by high resolution mass spectrometry analysis on a Waters I-class Acquity UPLC (Waters, UK) coupled with a Vion IMS QToF (Waters, UK) using a SeQuant ZIC-HILIC column (Merck, Germany). Detailed parameters of separation and spectrometry analysis were described previously (2). Data were acquired and processed using UNIFI 1.8.1. By analyzing the proportion of each isotopologue compared to the total levels, uptake rates of metabolite (glucose and glutamate) can be demonstrated.

LC-MS for Non-targeted Metabolites Analysis. Metabolites were extracted from adherent ADSCs and their differentiated adipocytes as previous methods described. Cells were scraped in ice-cold MeOH. Samples in 100 µl were mixed with 400 µl 80% aqueous solution containing MeOH, and vortex for 10 s, followed by centrifugation at 14,000 g for 20 min at 4 °C. The upper phase was collected and evaporated to dryness under vacuum. Samples were reconstituted in 100 µl double solvents for analysis. A pooled QC sample was mixed by equivalent parts from each prepared sample. Metabolites extracts were separated on a Vanquish UHPLC system (Thermo Fisher Scientific) equipped with an Accucore HILIC column (Thermo Fisher Scientific) kept at 40 °C. The chromatographic gradient was run at a flow rate of 0.3 ml/min. The LC flow was coupled to QE HF-X mass spectrometer (Thermo Fisher Scientific) with the scan range between 100-1,500 m/z. Normalized data set were uploaded to MetaboAnalyst for further analysis.

Statistical Analyses. Data were shown as mean ± SEM. The significance was determined by a one-way or two-way ANOVA with multiple comparisons, or a two-tailed unpaired Student t-test as appropriate with Prism software (GraphPad). * $p<0.05$, ** $p<0.01$ and *** $p<0.001$. The exact statistical parameters were presented in figure legends.

Figure S1

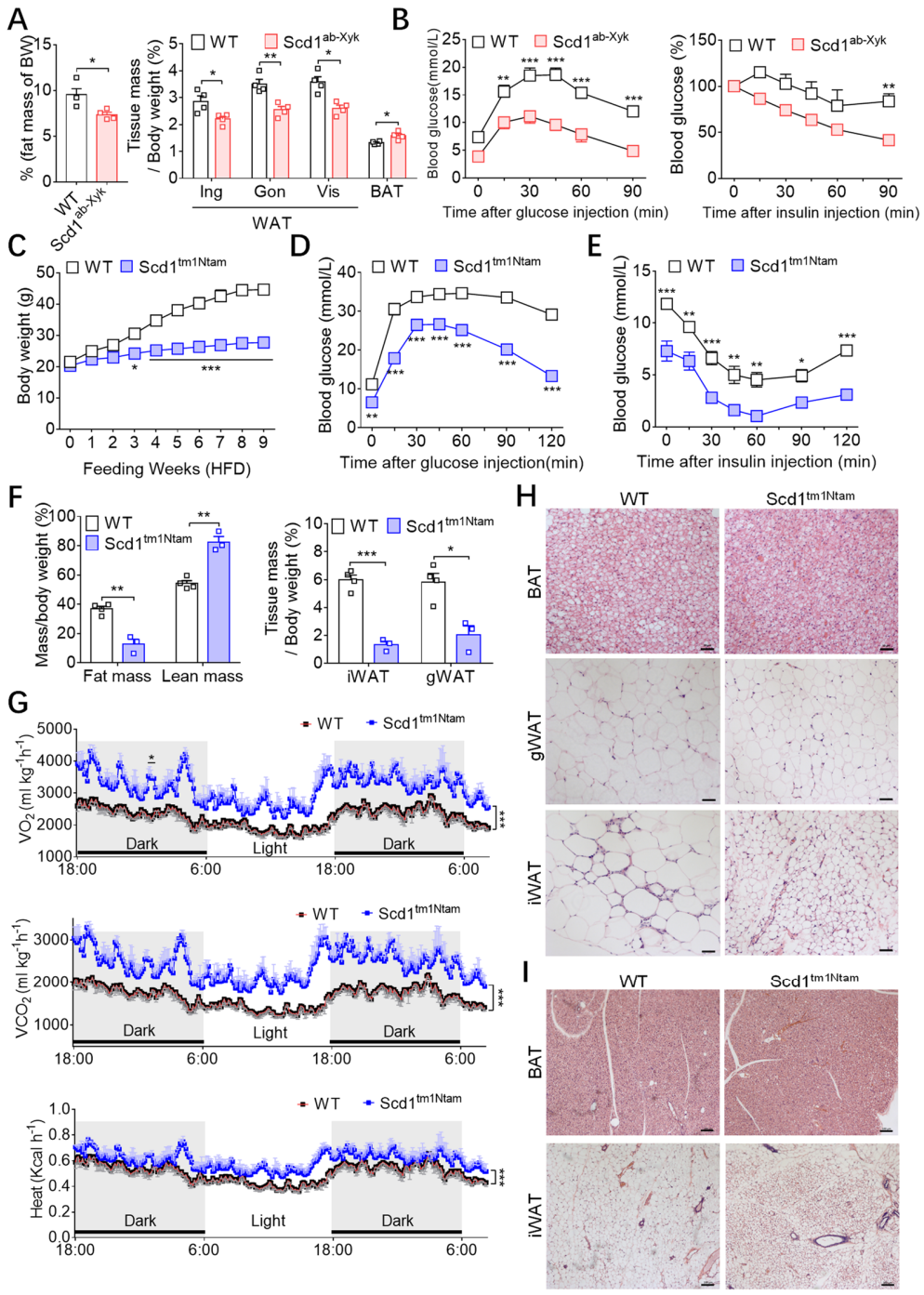

Fig. S1. Mice with Scd1 deficiency are resistance to HFD-induced obesity. (*A*) The ratio of total fat mass (left) or different adipose tissue mass (right) to body weight of WT and Scd1 mutant ($Scd1^{ab\text{-}Xyk}$) mice fed with an HFD for 10 weeks (n=4 for each group, repeated for two times). BW, body weight; Ing, inguinal; Gon, gonadal; Vis, visceral. (*B*) Glucose tolerance (left) and insulin sensitivity (right) of WT and Scd1 mutant ($Scd1^{ab\text{-}Xyk}$) mice fed with HFD (n≥3 for each group, repeated for two times). (*C*) Body weight of WT and Scd1 deficient ($Scd1^{tm1Ntam}$) mice with an

HFD for 9 weeks ($n \geq 3$ for each group, repeated for three times). (*D*-*E*) Glucose tolerance (*D*) and Insulin sensitivity (*E*) of WT and Scd1 deficient ($Scd1^{tm1Ntam}$) mice fed with HFD ($n \geq 3$ for each group, repeated for three times). (*F*) The ratio of fat mass and lean mass (left) and inguinal WAT (iWAT) and gonadal WAT (gWAT) (right) to body weight in WT and Scd1 deficient ($Scd1^{tm1Ntam}$) mice with HFD ($n \geq 3$ for each group, repeated for three times). (*G*) Daily O_2 consumption, CO_2 production and heat generation in WT and Scd1 deficient ($Scd1^{tm1Ntam}$) mice with an HFD monitored by metabolic cage ($n \geq 3$ for each group, repeated for two times). (*H*) H&E staining on representative sections of BAT, gWAT and iWAT from WT and Scd1 deficient ($Scd1^{tm1Ntam}$) mice with an HFD (scale bar, 50 μm). (*I*) Representative H&E staining of iWAT and BAT from 8-week old WT and Scd1 deficient ($Scd1^{tm1Ntam}$) mice (scale bar, 100 μm). Data are shown as Mean ± SEM. *$p < 0.05$, **$p < 0.01$ and ***$p < 0.001$.

Figure S2

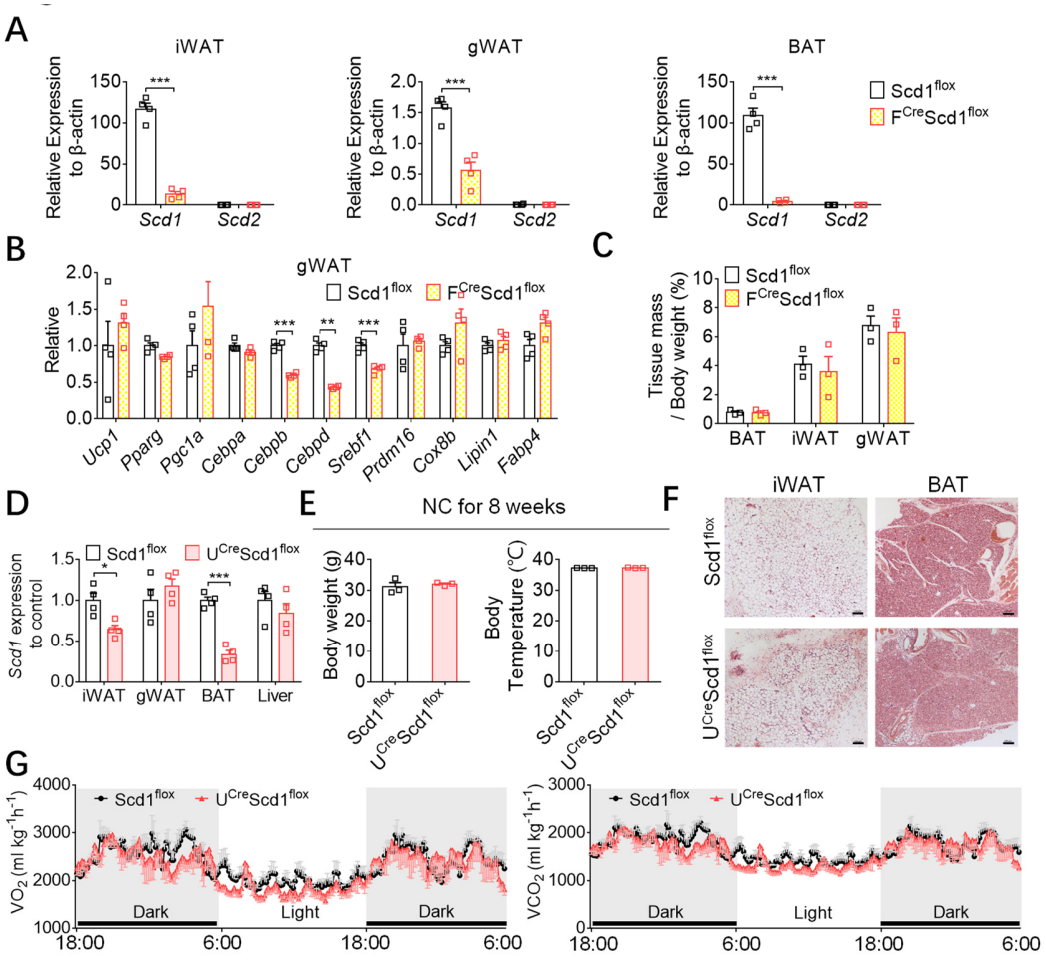

Fig. S2. Scd1 deficiency in white/brown adipocytes does not influence adipocyte composition and distribution. (*A*) The expression levels of *Scd1* and *Scd2* in iWAT, gWAT and BAT from 8-week old control ($Scd1^{flox}$) and $F^{Cre}Scd1^{flox}$ mice (*n*=4 for each group, repeated for two times). (*B*) Relative mRNA levels of thermogenesis and adipogenesis-related genes in gWAT of control ($Scd1^{flox}$) and $F^{Cre}Scd1^{flox}$ mice (*n*=4 for each group, repeated for two times). (*C*) The ratio of tissue mass to body weight in control ($Scd1^{flox}$) and $F^{Cre}Scd1^{flox}$ mice fed with an HFD (*n*=3 for each group, repeated for three times). (*D*) The relative mRNA expression level of *Scd1* in iWAT, gWAT, BAT, and Liver from 8-week old control ($Scd1^{flox}$) and $U^{Cre}Scd1^{flox}$ mice (*n*=4 for each group, repeated for two times). (*E*) The body weight (left) and rectal temperature (right) of control ($Scd1^{flox}$) and $U^{Cre}Scd1^{flox}$ mice fed a normal chow (NC) for 8 weeks (*n*=3 for each group, repeated for two times). (*F*) Representative H&E staining in iWAT and BAT from $U^{Cre}Scd1^{flox}$ and control ($Scd1^{flox}$) mice fed with NC for 8 weeks (scale bar, 100 μm). (*G*) Daily O_2 consumption and CO_2 production of control ($Scd1^{flox}$) and $U^{Cre}Scd1^{flox}$ mice fed with HFD (*n*=4 for each group, repeated for two times). Data are presented as Mean ± SEM. *p < 0.05, **p < 0.01 and ***p < 0.001.

Figure S3

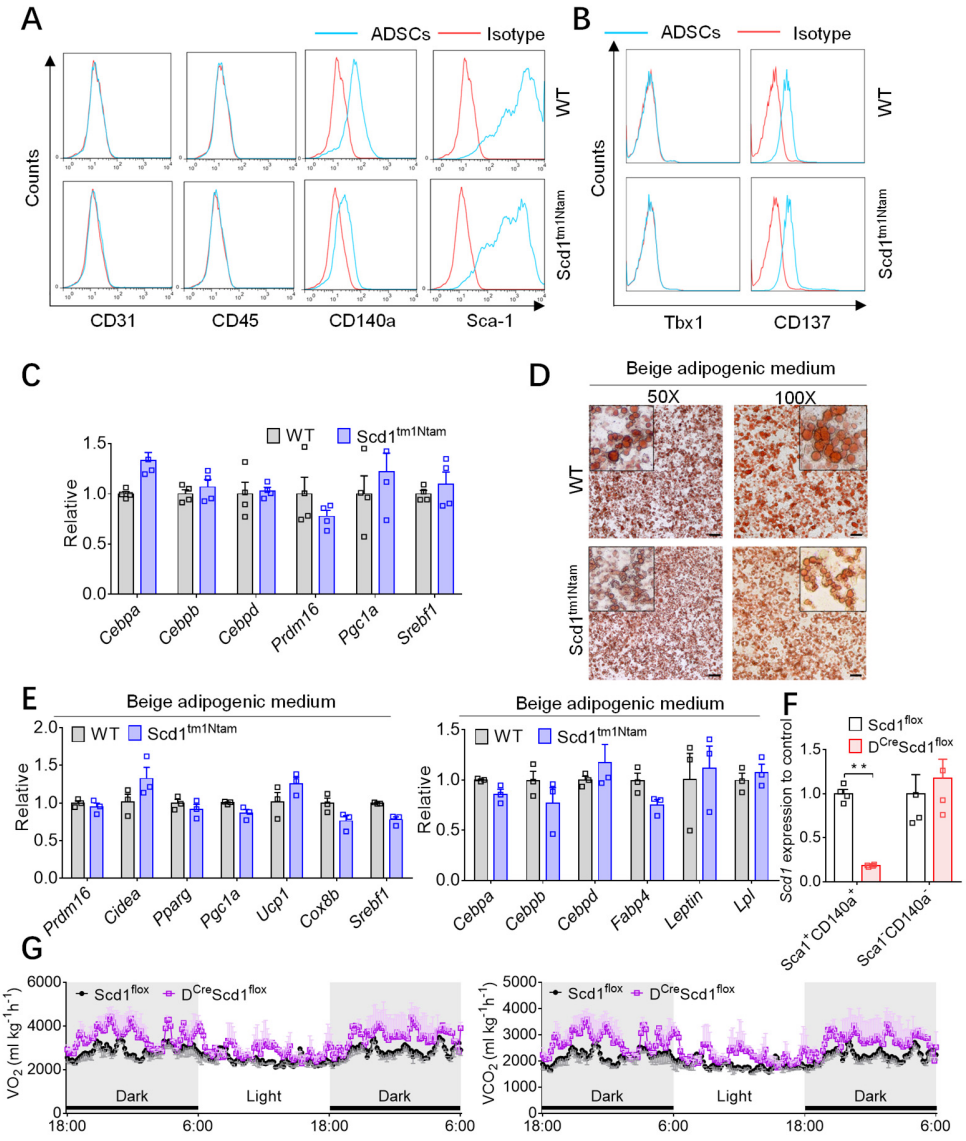

Fig. S3. Lack of Scd1 does not affect differentiation fate of ADSCs under beige adipogenic condition. (*A-B*) Phenotypical analysis of ADSCs isolated from WT and Scd1 deficient ($Scd1^{tm1Ntam}$) mice. The expressions of CD31, CD45, CD140a, Sca-1 (*A*), as well as TBX1 and CD137 (*B*) detected by flow cytometry. Blue, ADSCs; Red, isotype. (*C*) Relative expression of thermogenic and adipogenic genes in ADSCs from WT and Scd1 deficient ($Scd1^{tm1Ntam}$) mice (*n*=4 for each group, repeated for three times). (*D*) Oil red-O staining of ADSCs from WT and Scd1 deficient ($Scd1^{tm1Ntam}$) mice cultured in beige adipogenic medium for 7 days (50X, scale bar, 100 μm; 100X, scale bar, 50 μm). (*E*) Relative expression of genes associated with thermogenesis (left) and adipogenesis (right) in adipocytes generated from WT and Scd1 deficient ($Scd1^{tm1Ntam}$) ADSCs with beige adipogenic medium treatment (*n*=3 for each group, repeated for three times). (*F*) The relative expression level of *Scd1* in $Sca1^{+}CD140a^{+}$ preadipocytes and $Sca1^{-}CD140a^{-}$ cells sorted from $CD31^{-}CD45^{-}$ cells in stromal vascular fractions from iWAT of 8-week old control ($Scd1^{flox}$) and $D^{Cre}Scd1^{flox}$ mice (*n*=4 for each group, repeated for two times). (*G*) Daily O_2 consumption and CO_2 production of control ($Scd1^{flox}$) and $D^{Cre}Scd1^{flox}$ mice fed with HFD (*n*=3 for each group). Data are shown as Mean ± SEM. **p < 0.01.

Figure S4

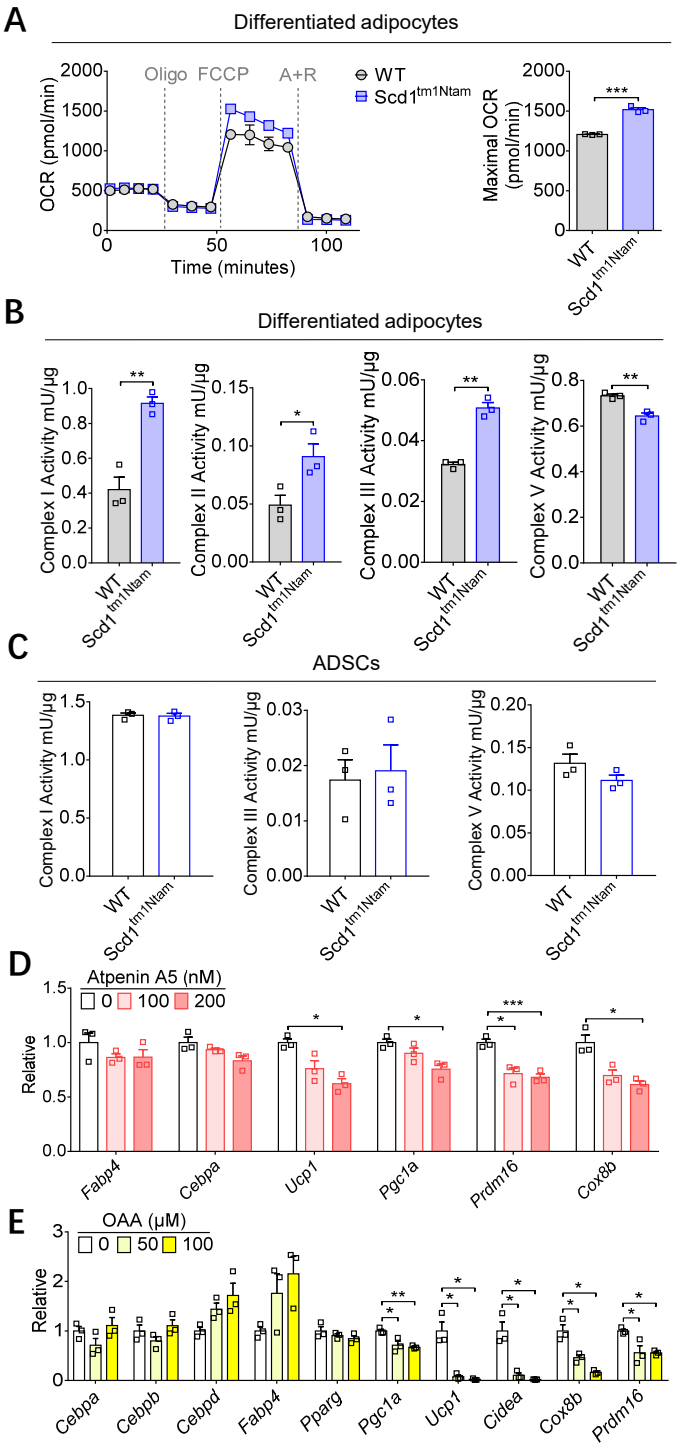

Fig. S4. Scd1 deficiency promotes beige adipogenesis of ADSCs through enhancing mitochondrial complex II activity. (*A*) The OCR (left) and maximal OCR (right) of differentiated adipocytes from WT and Scd1 deficient (Scd1^{tm1Ntam}) ADSCs under white adipogenic condition for 5 days (*n*=3 for each group, repeated for two times). (*B*) The activities of mitochondrial complex I,

II, III and V in adipocytes generated from WT and Scd1 deficient ($Scd1^{tm1Ntam}$) ADSCs (*n*=3 for each group, repeated for three times). (*C*) The activities of complex I, III and V per μg of mitochondrial protein in ADSCs derived from WT and Scd1 deficient ($Scd1^{tm1Ntam}$) mice (*n*=3 for each group, repeated for three times). (*D*) Relative expression of genes related to thermogenic adipogenesis in Scd1 deficient ($Scd1^{tm1Ntam}$) ADSCs cultured in white adipogenic condition and treated with or without Atpenin A5 for 7 days (*n*=3 for each group, repeated for three times). (*E*) Relative expression of genes associated with thermogenic adipogenesis in Scd1 deficient ($Scd1^{tm1Ntam}$) ADSCs cultured in white adipogenic condition and treated with or without oxaloacetic acid (OAA) for 7 days (*n*=3 for each group, repeated for three times). Data are shown as Mean ± SEM. *p < 0.05, **p < 0.01 and ***p < 0.001.

Figure S5

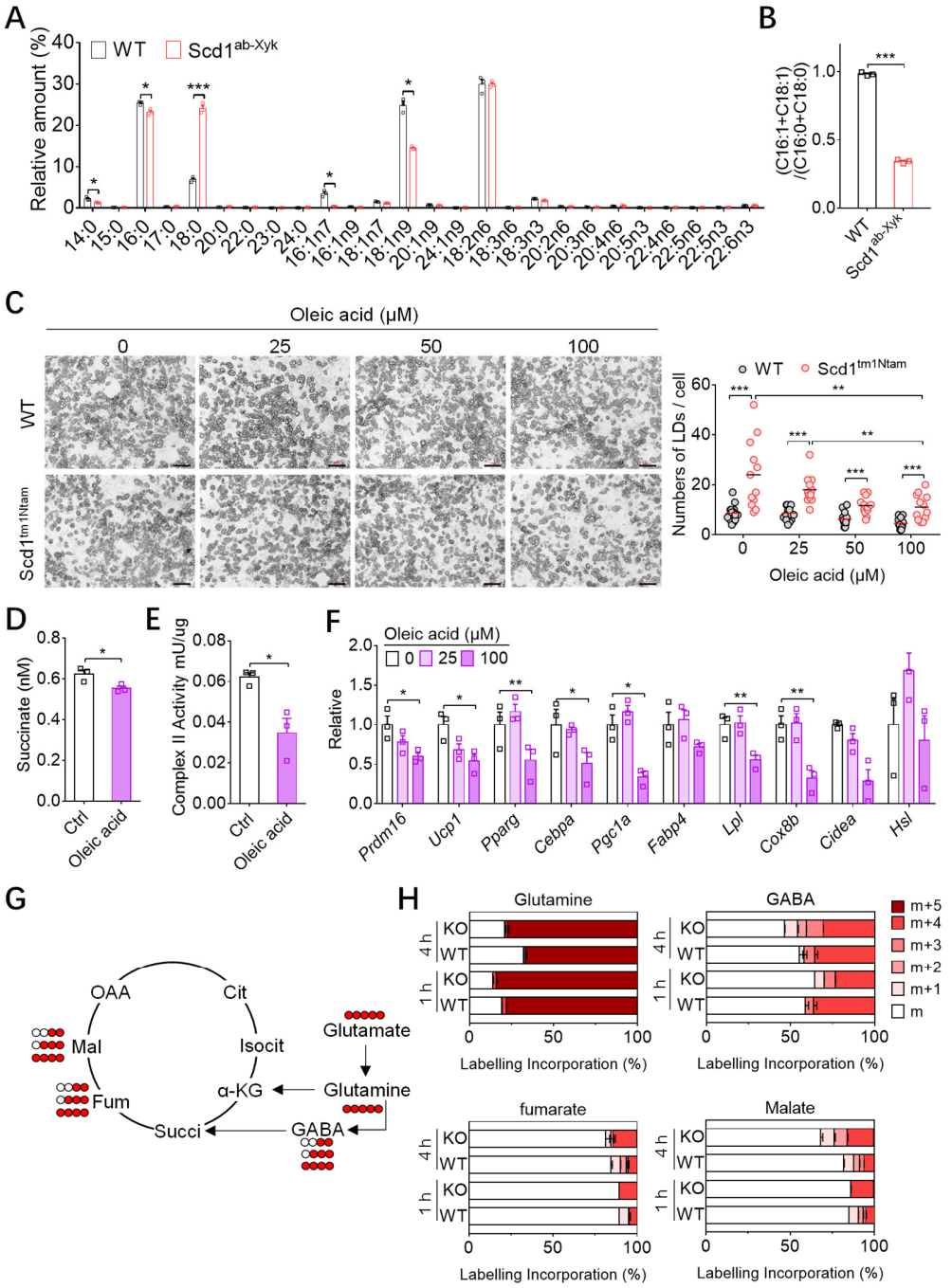

Fig. S5. Addition of oleic acid readjusts Scd1 deficient ADSCs to a white adipocyte differentiation. (*A*) Relative amount of fatty acids in iWAT of WT and Scd1 mutant (Scd1$^{ab\text{-}Xyk}$) mice calculated by GC/MS analysis (n=3 for each group, repeated for two times). (*B*) The ratio of monounsaturated fatty acids (C18:1 and C16:1) to saturated fatty acids (C18:0 and C16:0) in iWAT of WT and Scd1 mutant (Scd1$^{ab\text{-}Xyk}$) mice (n=3 for each group, repeated for two times). (*C*) Representative images (left) and the numbers of LDs per cell (right) of adipocytes generated from

WT and Scd1 deficient (Scd1^{tm1Ntam}) ADSCs under white adipogenic condition, with the treatment of oleic acid at concentrations of 0, 25, 50, 100 μM respectively (scale bar, 100 μm, n≥12 for each group, repeated for three times). (*D-E*) The concentration of succinate (*D*) and the activity of mitochondrial complex II (*E*) in adipocytes generated from Scd1 deficient (Scd1^{tm1Ntam}) ADSCs, along with or without (Ctrl) oleic acid (100 μM) treatment (n=3 for each group, repeated for two times). (*F*) Relative expression of genes associated with thermogenesis and adipogenesis in Scd1 deficient (Scd1^{tm1Ntam}) ADSCs cultured in white adipogenic condition and treated with or without oleic acid for 7 days (n=3 for each group, repeated for three times). (*G*) Schematic illustration of ^{13}C tracing of [U-^{13}C]-glutamate in TCA cycle. (*H*) Adipocytes generated from WT and Scd1 deficient ADSCs (Scd1^{tm1Ntam}, KO) were incubated with [U-^{13}C]-glutamate for 1 or 4 hours (h). After extracting polar metabolites, the labelling proportion of each isotopologue in the total were calculated (n=5 for each group). Data are shown as Mean ± SEM. *p < 0.05, **p < 0.01 and ***p < 0.001.

Figure S6

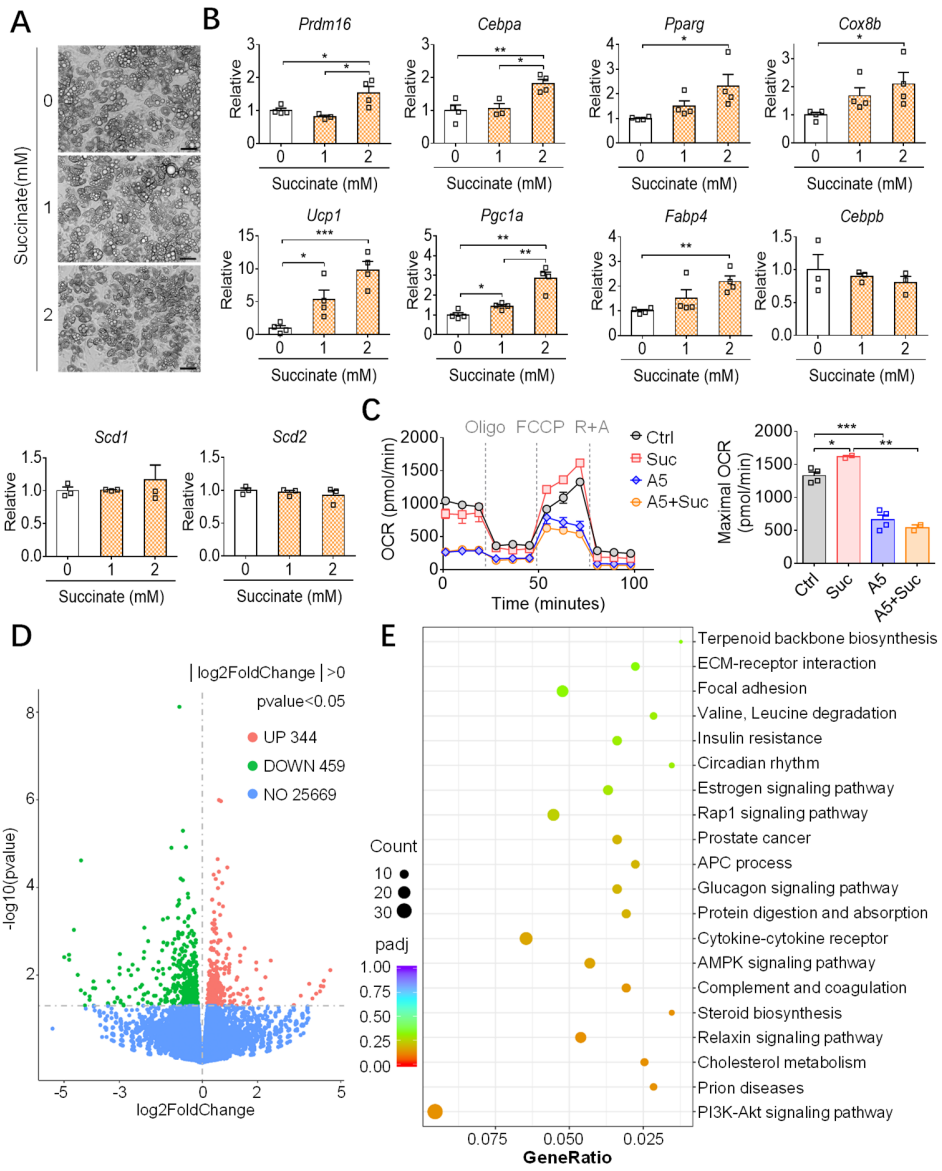

Fig. S6. Addition of succinate induces beige adipogenesis *in vitro*. (*A*) Representative images of WT ADSCs cultured in white adipogenic medium, with or without succinate (1 mM and 2 mM) treatment for 7 days (scale bar, 100 μm). (*B*) Relative expression of genes associated with thermogenesis and adipogenesis in adipocytes differentiated from WT ADSCs, with or without succinate (1 mM and 2 mM) treatment ($n \geq 3$ for each group, repeated for three times). (*C*) The OCR (left) and the maximal OCR (right) of adipocytes generated from ADSCs, with or without the treatment of succinate (Suc, 2 mM), Atpenin A5 (A5, 100 nM) or their combinations. (*D*) Volcano plot of RNA-seq data from adipocytes differentiated from WT ADSCs with or without succinate treatment (2 mM). (*E*) Dot plot showing the top 20 most significantly enriched KEGG pathways for the differentially regulated transcripts between succinate treated and untreated differentiated adipocytes from WT ADSCs. The color of the dot represents p value and size of the dot represents the number of differentially regulated transcripts mapped to the reference pathways. Data are shown as Mean ± SEM. *p < 0.05, **p < 0.01 and ***p < 0.001.

Figure S7

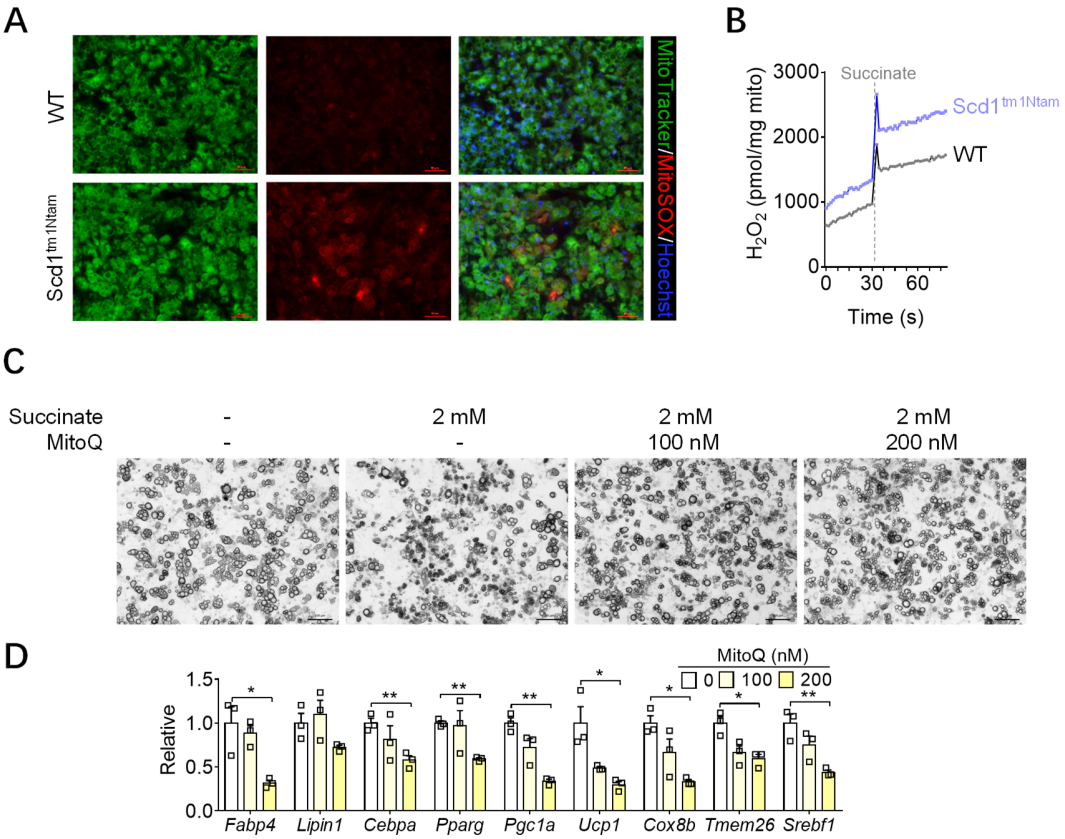

Fig. S7. **Scd1 deficiency enhances the production of mitochondrial reactive oxygen species during adipogenesis.** (*A*) Representative images of MitoSOX Red and Mito-Tracker Green in adipocytes generated from WT and Scd1 deficient ($Scd1^{tm1Ntam}$) ADSCs (scale bar, 50 μm). (*B*) H_2O_2 emission by mitochondria (mito) from WT or Scd1 deficient ($Scd1^{tm1Ntam}$) adipocytes, with succinate (10 mM) addition. (*C*) Representative images of adipocytes differentiated from WT ADSCs treated with succinate (2 mM) alone or combined with mitoquinone (mitoQ, 100 nM, 200 nM) for 7 days (scale bar, 100 μm). (*D*) Relative expression levels of genes associated with adipogenesis in WT ADSCs cultured under the white adipogenic condition for 7 days, treated with succinate (2 mM) alone or combined with mitoquinone (mitoQ, 100 nM, 200 nM) (n=3 for each group, repeated for two times). Data are shown as Mean ± SEM. *p < 0.05 and **p < 0.01.

Figure S8

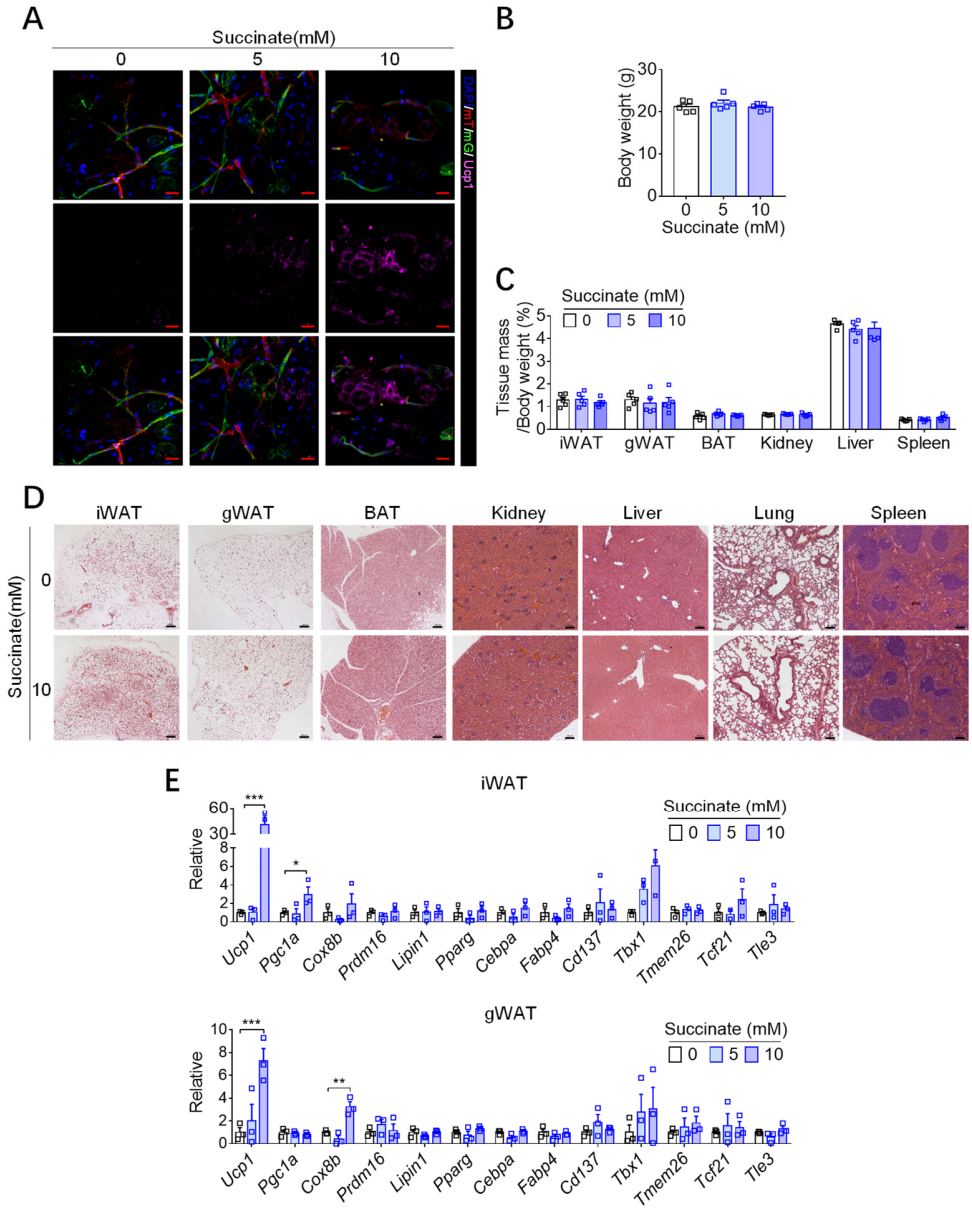

Fig. S8. Supplementation of succinate promotes beige adipocytes formation *in vivo*. (*A*) Representative images of Ucp1 in implants by whole mount staining. Green, EGFP; red, tdTomato; purple, Ucp1; blue, DAPI. Scale bar, 20 μm. (*B-C*) Body weight (*B*) and the ratio of tissue mass to body weight (*C*) of mice with or without succinate (5 mM and 10 mM) treatment for 4 weeks (*n*=5 for each group, repeated for two times). (*D*) Representative H&E staining of iWAT, gWAT, BAT, kidney, liver, lung and spleen in mice with or without succinate (10 mM) treatment for 4 weeks (scale bar, 100 μm). (*E*) Relative expression of genes associated with thermogenesis and adipogenesis in iWAT and gWAT of mice, with or without succinate treatment for 4 weeks (*n*=3 for each group, repeated for two times). Data are shown as Mean ± SEM. *p < 0.05, **p < 0.01 and ***p < 0.001.

Table S1. Primers information.

Gene names	Primer Details
m*Actβ*-F	GGCTGTATTCCCCTCCATCG
m*Actβ*-R	CCAGTTGGTAACAATGCCATGT
m*Scd1*-F	TTCTTGCGATACACTCTGGTGC
m*Scd1*-R	CGGGATTGAATGTTCTTGTCGT
m*Scd2*-F	GCATTTGGGAGCCTTGTACG
m*Scd2*-R	AGCCGTGCCTTGTATGTTCTG
m*Fabp4*-F	AAGGTGAAGAGCATCATAACCCT
m*Fabp4*-R	TCACGCCTTTCATAACACATTCC
m*Lpl*-F	GGGAGTTTGGCTCCAGAGTTT
m*Lpl*-R	TGTGTCTTCAGGGGTCCTTAG
m*Cidea*-F	TGACATTCATGGGATTGCAGAC
m*Cidea*-R	GGCCAGTTGTGATGACTAAGAC
m*Cox8b*-F	TGTGGGGATCTCAGCCATAGT
m*Cox8b*-R	AGTGGGCTAAGACCCATCCTG
m*Prdm16*-F	CCCCACATTCCGCTGTGAT
m*Prdm16*-R	CTCGCAATCCTTGCACTCA
m*Srebf1*-F	GCAGCCACCATCTAGCCTG
m*Srebf1*-R	CAGCAGTGAGTCTGCCTTGAT
m*Ucp1*-F	AGGCTTCCAGTACCATTAGGT
m*Ucp1*-R	CTGAGTGAGGCAAAGCTGATTT
m*Cd137*-F	CGTGCAGAACTCCTGTGATAAC
m*Cd137*-R	GTCCACCTATGCTGGAGAAGG
m*Tbx1*-F	GGCAGGCAGACGAATGTTC
m*Tbx1*-R	TTGTCATCTACGGGCACAAAG
m*Tmem26*-F	ACCCTGTCATCCCACAGAG
m*Tmem26*-R	TGTTTGGTGGAGTCCTAAGGTC
m*Tcf21*-F	AGATCCCACCTCAAACCCAACACA
m*Tcf21*-R	TGTTGGAGTCCACTTTCAGGGAGT
m*Tle3*-F	TGGTGAGCTTTGGAGCTGTT
m*Tle3*-R	CGGTTTCCCTCCAGGAAT
m*Cebpa*-F	CAAGAACAGCAACGAGTACCG
m*Cebpa*-R	GTCACTGGTCAACTCCAGCAC
m*Cebpb*-F	CACCCGCGTTCATGCAACG
m*Cebpb*-R	CCGCCTCGTAGTAGAAGTTGGC
m*Cebpd*-F	CCCGCCATGTACGACGACGAGAG
m*Cebpd*-R	GAAGAGGTCGGCGAAGAGCTCGT
m*Pparg*-F	TCGCTGATGCACTGCCTATG
m*Pparg*-R	GAGAGGTCCACAGAGCTGATT
m*Leptin*-F	GAGACCCCTGTGTCGGTTC
m*Leptin*-R	CTGCGTGTGTGAAATGTCATTG
m*Pgc1a*-F	TATGGAGTGACATAGAGTGTGCT
m*Pgc1a*-R	CCACTTCAATCCACCCAGAAAG
m*Lipin1*-F	CTCCGCTCCCGAGAGAAAG
m*Lipin1*-R	TCATGTGCAAATCCACGGACT

Dataset S1 (separate file). Metabolomics details related to Fig. 5 *A* and *B*.

Dataset S2 (separate file). Betweenness centrality value related to Fig. 5*D*.

Dataset S3 (separate file). Identification information related to Fig. 5 G and H, Fig. 5S G and H.

SI References

1. Zheng C*, et al.* (2015) CD11b regulates obesity-induced insulin resistance via limiting alternative activation and proliferation of adipose tissue macrophages. *Proc Natl Acad Sci U S A* 112(52):E7239-7248.
2. Yao R*, et al.* (2018) Engineering and systems-level analysis of Pseudomonas chlororaphis for production of phenazine-1-carboxamide using glycerol as the cost-effective carbon source. *Biotechnol Biofuels* 11:130.